Modeling and Investigation of Vertical Laminar Airflow with Perimeter Air Curtain Ventilation System in Surgical Site of Hospital Using Computational Fluid Dynamics

S B Thool[1], S L Sinha[2]
Department of Mechanical Engineering
[1]Rungta College of Engineering and Technology, Bhilai, India
sbthool@rediffmail.com
[2] National Institute of Technology, Raipur, India
shobha_sinha1@rediffmail.com

ABSTRACT: Traditionally vertical laminar flow system has been preferred for infection control due to airborne contaminants. This arrangement requires high air change rates based on the size of the treated area. Because of mixing at the boundary of the air piston, the perimeter of laminar flow panel array should be sized to extend beyond the critical work envelope by at least 15 cm.

In order to limit the total area of laminar flow panel array and Air Change per Hour, a hybrid air distribution system utilizing the benefits of laminar system and ideally included continuous perimeter air curtain around an interior laminar flow panels has been studied using computational fluid dynamics and has been compared against the traditionally used vertical laminar system without air curtain.

The results shows that the perimeter flow is typically in the form of a narrow “shealth” of higher velocity air acted as a protective barrier that prevents the re-entering of contaminated air into the laminar flow.

Keywords: Laminar ventilation, Air Curtain, Infection control, Operating Room, CFD.

1. INTRODUCTION

Vertical flow applications consisting of an array of ceiling laminar flow panels strategically located just over the critical work envelope are often utilized in operating/surgical sites and similarly critical areas in health care facilities [1]. It is generally accepted that a properly installed and operated system, providing a clean source of supply air, will reduce the incidence of infections due to airborne contaminants. This arrangement is preferred where an entire ceiling array is not practical, but can still require high air change rates based on the size of the treated area [2]. Because of mixing at the boundary of the air piston, the perimeter of laminar flow panel array should be sized to extend beyond the critical work envelope by at least 15 cm.

Hybrid air distribution systems have evolved utilizing the benefits of laminar systems and ideally include a continuous perimeter air curtain around an interior laminar flow panels (Fig. 1), essentially creating a “space within a space”. This system consists of two or more laminar flow diffusers located over the operating room table surrounded by a low velocity air curtain created by a special slot diffuser. Typically, two-thirds of the supply airflow is directed through the perimeter curtain and the remaining one third directed through the laminar flow diffusers over the operating table [3]. These systems typically require lower overall air change rates (15 – 150 ACH) for the space, with higher air change rates resulting in the cube within the air curtain. With lower air exchange rates commonly being specified it becomes the system of choice for most operating room applications. A vertical laminar flow with air curtain system is also more friendly to design as it provides only one third of its volume through the center panels, which are usually uniformly spaced within the air curtain and over the operating table. This allows the prediction of much more accurate estimates of throw velocity as the manufacture’s standard data can be used with corrections for temperature and spacing [4].

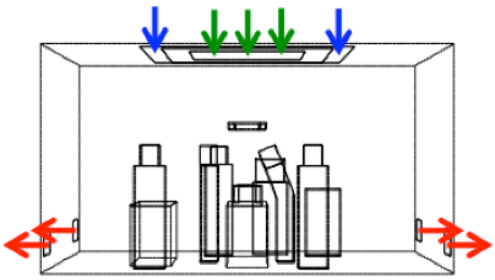

Fig. 1 Vertical Laminar Ventilation system with Air Curtain

2 CFD MODELING

2.2 The Turbulent Airflow Model

The present study has been carried out using Eulerian method to simulate the airflow field. The interaction between fluid phase and discrete phase is assumed to be one way, and the impact from discrete phase to fluid phase is negligible. This is feasible since the particle volume fraction is sufficiently small. Thus the airflow field is independent on the particulate phase and could be determined in advance.

In order to model the random feature of turbulent flows, a time decomposition (also called Reynods decomposition) of the instantaneous flow variables ϕ(t) is introduced into the governing equations of the flow field. The turbulent viscosity arising out of this random feature of turbulent flows is commonly obtained by solving the two additional transport equation in addition to mass, momentum and energy conservation equations. The *k*-*ε* model is the most popular turbulence model, in which transport equations are solved for the turbulent kinetic energy *k*, and its dissipation *ε*.

The general governing equation for airflow is as follows (Patankar, 1980) [5].

$$\frac{\partial(\rho\phi)}{\partial t}+\frac{\partial(\rho V\phi)}{\partial x}+\frac{\partial(\rho V\phi)}{\partial y}+\frac{\partial(\rho V\phi)}{\partial z}=\frac{\partial}{\partial x}\left[\mathcal{T}_\phi\frac{\partial\phi}{\partial x}\right]+\frac{\partial}{\partial y}\left[\mathcal{T}_\phi\frac{\partial\phi}{\partial y}\right]+\frac{\partial}{\partial z}\left[\mathcal{T}_\phi\frac{\partial\phi}{\partial z}\right]+S_\phi \quad \text{.....(1)}$$

Flow variables, expressions for the effective diffusivity, Γ_ϕ; and source term, S_ϕ for each variable for continuity, momentum and energy equation are described by Launder and Spalding [6].

Continuity Equation:

$\phi = 1;\qquad \Gamma_\phi = 0;\ S_\phi = 0$

Momentum Equation:

$\phi = u,\quad \Gamma_\phi = \nu + \nu_T \quad S_\phi = -\frac{1}{\rho}\frac{\partial p}{\partial x} + S'_u,$ (u-momentum equation)

$\phi = v,\quad \Gamma_\phi = \nu + \nu_T \quad S_\phi = -\frac{1}{\rho}\frac{\partial p}{\partial y} + S'_v,$ (v-momentum equation)

$\phi = w,\quad \Gamma_\phi = \nu + \nu_T \quad S_\phi = -\frac{1}{\rho}\frac{\partial p}{\partial z} + S'_w,$ (w-momentum equation)

Energy Equation:

$\phi = T;\ \Gamma_\phi = \frac{\nu}{Pr} + \frac{\nu_T}{Pr_T};\quad S_\phi = S_T;$

Turbulent quantities:

$\phi = k;\ \Gamma_\phi = \frac{\nu_T}{\sigma_k}\ ;\ S_\phi = P - D,\ \frac{\varepsilon}{k}(C_{\varepsilon 1}P - C_{\varepsilon 2}D)$ (Turbulent kinetic energy equation)

$\phi = \varepsilon;\ \Gamma_\phi = \frac{\nu_T}{\sigma_\varepsilon};\ S_\phi = \frac{\varepsilon}{k}(C_{\varepsilon 1}P - C_{\varepsilon 2}D)$ (Dissipation rate equation)

where,

$$P = 2\nu_T\left[\left(\frac{\partial u}{\partial x}\right)^2+\left(\frac{\partial v}{\partial y}\right)^2+\left(\frac{\partial w}{\partial z}\right)^2\right]+\nu_T\left[\left(\frac{\partial u}{\partial y}+\frac{\partial v}{\partial x}\right)^2+\left(\frac{\partial v}{\partial z}+\frac{\partial w}{\partial y}\right)^2+\left(\frac{\partial w}{\partial x}+\frac{\partial u}{\partial z}\right)^2\right] \text{ and } D = \varepsilon$$

The CFD program solves above equations in the form of discretized algebraic equations. The second-order upwind scheme for discretization has been used for all variables except the pressure term. For pressure, a staggered scheme called PRESTO has been selected from FLUENT software [7]. Finally, this study uses the SIMPLE algorithm [5] to couple pressure and velocity.

2.3 Equations for Particle Motion and Dynamics

The Lagrangian particle tracking method has been used to calculate individual trajectories by solving the momentum equation. Particles motion in carrier fluid is affected by various forces such as viscous drag force, gravity force, added mass force (virtual mass force), Brownian force, and pressure force. In this study, Brownian force has been ignored due to the large size of particle. The added mass force is considered in a few simulations and is found to have negligible influence on particle trajectory [8]. Thus in this study, steady viscous drag force, gravity force and pressure force have been considered. The final form of the trajectory equations are given as under:

$$m_p \frac{du_p}{dt} = \frac{1}{2} C_D A_p \rho (u - u_p) \sqrt{(u - u_p)^2 + (v - v_p)^2 + (w - w_p)^2} + m_p g_x \quad \text{.....(2)}$$

$$m_p \frac{dv_p}{dt} = \frac{1}{2} C_D A_p \rho (v - v_p) \sqrt{(u - u_p)^2 + (v - v_p)^2 + (w - w_p)^2} + m_p g_y \quad \text{.....(3)}$$

$$m_p \frac{dw_p}{dt} = \frac{1}{2} C_D A_p \rho (w - w_p) \sqrt{(u - u_p)^2 + (v - v_p)^2 + (w - w_p)^2} + m_p g_z \quad \text{.....(4)}$$

where,

u, v, w	-	instantaneous velocity of air in *x*, *y* and *z* directions respectively;
u_p, v_p, w_p	-	particle velocity in *x*, *y* and *z* directions respectively;
x_p, y_p, z_p	-	movement of particle in *x*, *y* and *z* direction respectively;
g_x, g_y, g_z	-	acceleration due to gravity in *x*, *y* and *z* directions respectively;
A_p	-	cross-sectional area of the particle;
m_p	-	mass of particle;
ρ	-	density of the particle;
C_D	-	drag coefficient;
dt	-	time interval

$C_D = \frac{24}{Re}\left(1 + \frac{3}{16} Re\right)^{0.5}$ for $Re \leq 560$

and

$C_D = 0.44$ for $Re > 560$

The Reynolds number of the particle is based on the relative velocity between particle and air. The time-averaged flow field determined the mean path of particles, while the instantaneous flow field governed each particle's turbulent dispersion from the mean trajectory. The present investigation used the discrete random walk (DRW) model to simulate the stochastic velocity fluctuations in the airflow. The DRW model assumes that the fluctuating velocities follow a Gaussian probability distribution. The fluctuating velocity components, $\vec{V}$ have the following form:

$$\vec{V}' = \zeta \sqrt{2k/3} \quad \text{……...(5)}$$

where, k is the turbulent kinetic energy and ζ is the normally distributed random number. The term $\bar{V}'$remains constant during each time step. The time step was chosen so that a particle remains in the same local eddy within each particular time slot. By replacing the mean velocity components $\vec{V} = \bar{V} + \vec{V}'$ in Eq. (2), (3), (4), each trajectory could then interact with the modeled flow field at each instance in time.

Assuming isotropic turbulence, the instantaneous velocity of air are then calculated from kinetic energy of turbulence:

$$u = \bar{u} + N\alpha; \qquad v = \bar{v} + N\alpha; \quad w = \bar{w} + N\alpha \quad \text{…….. (6)}$$

Where N is the pseudo-random number, ranging from 0 to 1, with

$$\alpha = \left(\frac{2k}{3}\right)^{0.5} \quad \text{.....(7)}$$

Where k is the turbulent kinetic energy.

The mean velocity, which are the direct output of CFD, determine the convection of the particles along the streamline, while the turbulent fluctuating velocity, $N\alpha$, contributes to the turbulent diffusion of the particle.

3 Brief of Operating Room

In a typical operating room layout five surgical staff members, lights, machinery, tables and patient have been considered for the baseline model for the CFD simulations. The brief description of operating room is given in the Fig. 2 and Table 1. The array of supply grilles immediately above the table is 1.83 m x 1.83 m in size. Air curtains on all four sides are of 0.6 m wide. The most suitable operating value of ACH for this system is ranging from 25 h^{-1} to 30 h^{-1}. The present CFD simulation is done taking ACH as 27.45 h^{-1} and air velocity from main grilles as 0.14 m/s and velocity from air curtains as 0.28 m/s with temperature as 27 C°.

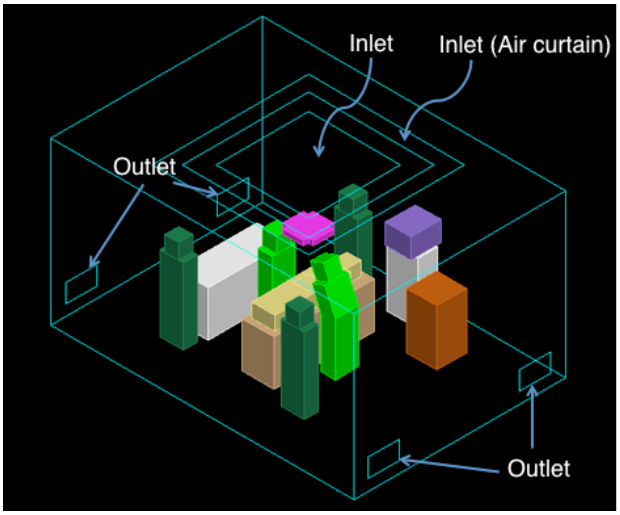

Fig. 2 Baseline model of the operating room

Table 1
Dimension of operating room and other available items

Item	Dimensions
Operating table	0.64 m x 2.0 m x 0.9 m
Surgical lamp	0.55 m x 0.55 m x 0.1 m
Anesthesia machine	0.6 m x 0.6 m x 1.1 m
Back table	0.64 m x 1.6 m x 0.9 m
Monitor stand	0.6 m x 0.5 m x 1.20 m
Monitor	0.5 m x 0.4 m x 0.6 m
Surgical staff (Two surgeon and three nurses)	0.46 m x 0.28 m x 1.8 m each
Patient	0.46 m x 0.28 m x 1.8 m

3 BOUNDARY CONDITIONS

The velocity, temperature and turbulent transport quantities over the inlet boundary are prescribed from the experimental data found by Memarzadeh and Manning [9]. The velocity of air from the central laminar airflow inlet is taken as 0.14 m/s and that from the air curtain panels as 0.28 m/s as per the criteria mentioned above. Outlet boundary conditions are set as the Neumann boundary condition. No slip boundary condition has been used at the wall. Wall functions have been applied to describe the turbulent flow properties in the near wall region.

The initial conditions for particle tracking include the starting position and initial velocities of particles. For this study, the particles are assumed to have the density of the oil smoke particle, i.e. $\rho_P = 850$ kg/m^3. Particles are assumed to have diameter of 15 microns [9]. Other boundary conditions regarding the rate of generation of contaminant particles, heat generations from equipment and human bodies have been illustrated in Fig. 3.

When particles reach air supply inlets or exhaust outlets, they will escape and the trajectories terminate. When reaching a rigid object, particles may either attach to or rebound from the object's surface. Particles in a ventilated room are most likely to attach to the surface since they usually cannot accumulate enough rebound energy to overcome adhesion [10]. It is therefore natural to terminate, or "trap", a particle trajectory after hitting a rigid surface. This treatment was adopted and used in many CFD studies of the indoor environment.

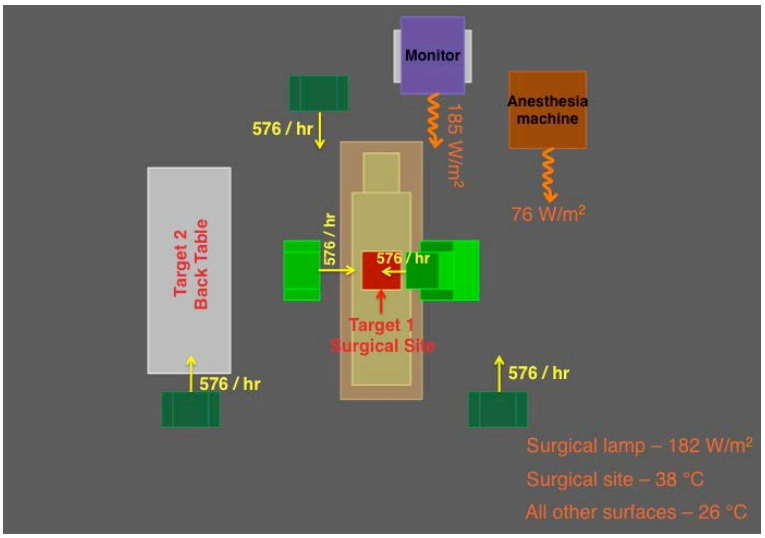

Fig. 3 Heat and Particle Generation Rate

4. PARTICLE TRACKING

The methodology is refined to consider different particle outcomes, namely:

- The particle is vented from the room via ventilation and
- The particle hits one of the two designated targets, namely, the surgical site (patient body put under surgery) or the top surface of the back table.

Particles that are neither vented nor strike the target are assumed to remain in the room when the overall particle tracking time limit (1 hour in present case) is reached.

6. MODELING PROCEDURES

The CFD solver FLUENT 6.0 [6] has been used to numerically solve the Navier-Stokes equations. This solver has a finite volume solution scheme for the mean momentum, energy, and turbulent transport equations. As part of the same package, a pre-processor GAMBIT [11] is used to generate the required grid for the solver. An unstructured grid with rectangular elements is used. The whole surgical site domain has been divided into 629762 equally spaced elements as shown in figure 5. The turbulence model used in this work is based on a two-equation model (i.e., a standard k-ε model from Launder and Spalding[6]). Incompressible flow is assumed; thus the use of a segregated solver is adequate. The second-order upwind implicit schemes have been selected to perform computations. The SIMPLE method [5] has been selected to solve the pressure-velocity coupling.

Particle tracking for turbulent dispersion of particles in a turbulent flow is calculated by using stochastic model of FLUENT 6.0. Number of tries of particle tracking was set to 8 to get the representative number of 512 particles released from each source since surface element size was having 64 elements generating each particle.

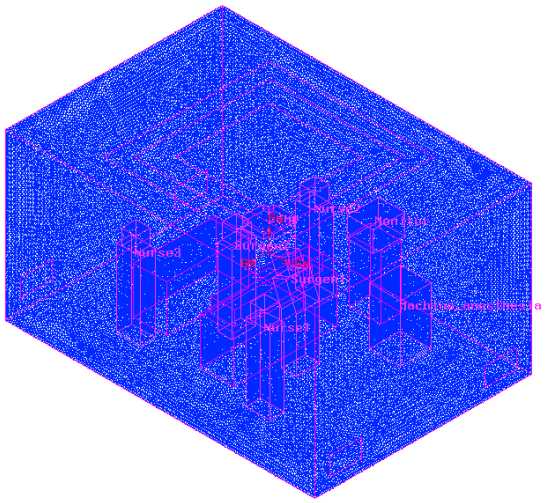

Fig. 4 Mesh used for the operating room

7. Results and Discussion

The numerical simulation results obtained by FLUENT software are shown in Fig. 5 in the form of path lines, velocity distribution and velocity contours. It has been clearly observed that the interior “cube” formed by the air curtain maintains a positive pressure relationship compared to the exterior or surrounding area outside the air curtains. This results in high to low-pressure particle movement. Particulate movement from the critical envelope down along the floor and out of the space represents the shortest path

for removal. The air quantity extracted from the space through these grilles determines the room pressure and the pressure relationship of the space with respect to adjacent spaces, either positive (ex-filtration or low flow into the space from an adjacent space), or neutral. It has been again observed that there is a formation of predictable, repeatable velocity differential between the laminar flow and a specialized flow. The perimeter flow is typically in the form of a narrow “shealth” of higher velocity air and it is acted as a protective barrier that prevents re-entering contaminated air into the laminar flow. Its main function is “acting as continual exhaust”. And this causes it to make laminar behave better.

Table 2 shows the performance of the laminar ventilation system with perimeter air curtain against the traditional one in terms of number of particle escaped from the room, number of particle struck on the Site of Surgery and number of particle struck on the surface of Back Table. Results show that the number of contaminated particles mainly generated from the nurses escaped from the operating room, in case of ventilation system with air curtain is more as compared to the system without air curtain. This is due to fact that the re-entering of particles from the outer part of critical area is hurdled by the air curtain.

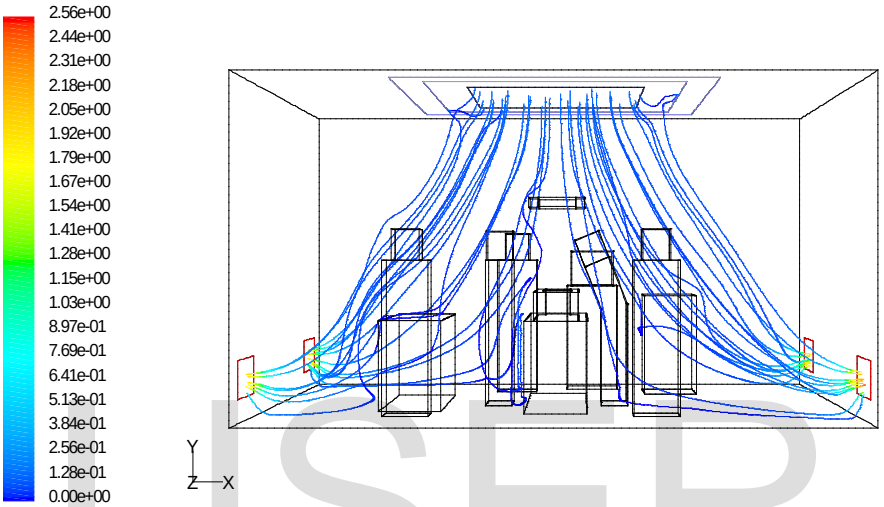

(a) Air Flow Field Pattern

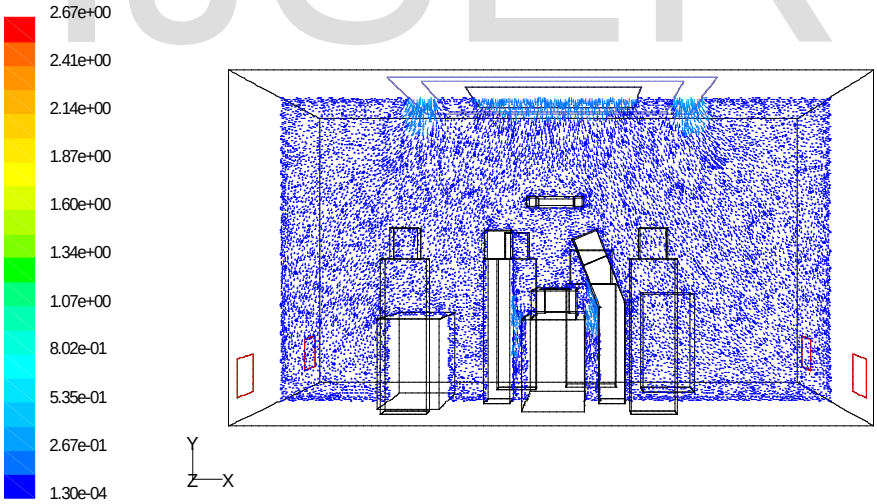

(b) Velocity Distribution (at vertical plane at z = 0)

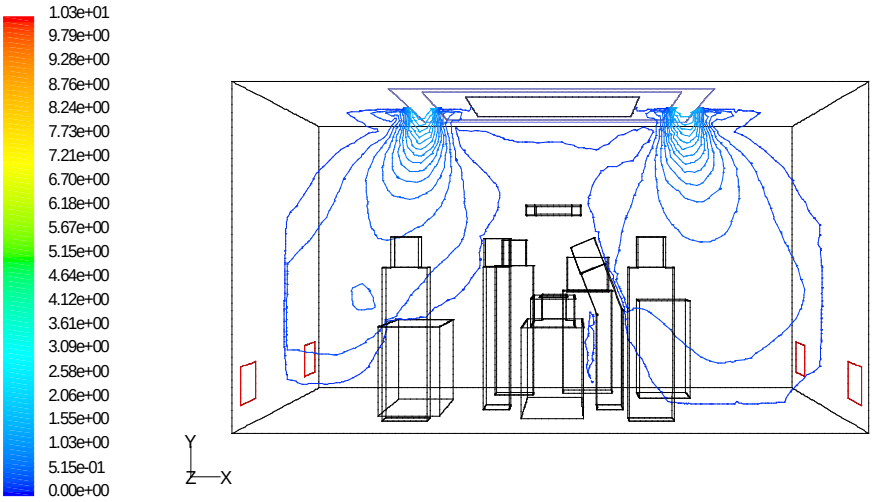

(c) Velocity Contours (at vertical plane at z = 0)

Fig. 5 Numerical Simulation Results

Table 2

Percentage of Particles Vented from Room and Percentage of Particles Strike on Surgical Site and Back Table for Laminar Ventilation System without air curtain and with air curtain

Laminar Ventilation Systems	Particle Source	Total Number of particles released	Contaminated particles escaped from Operating Room		Contaminated Particles Strike on Surgery Site		Contaminated Particles Strike on Back Table	
			Nos.	%	Nos	%	Nos	%
Without air curtain	Surgeons	512*2 = 1024	891	87.1	1	0.10	1	0.10
	Nurse	512*3 = 1536	816	53.1	0	0.00	4	0.26
With air curtain	Surgeons	512*2 = 1024	945	93.2	1	0.10	1	0.10
	Nurses	512*3 = 1536	1519	98.9	0	0.00	0	0.00

References

[1] Hospital Infection Control Practices Advisory Committee, Recommendations for isolation precautions in hospitals. American Journal of Infection Control 24: 24 – 52, (1996).

[2] Gerald Cook, Air Motion Control in the Hospital Operating Room, ASHRAE Journal, 30 – 39, (2009).

[3] ASHRAE, HVAC Design Manual for Hospitals and Clinics, (2003).

[4] Int-Hout, D., Cook. G., A new idea that is 40 years old—air curtain hospital operating rooms systems, *ASHRAE Transactions* 113(1) (2006).

[5] Patankar S. V., Numerical Heat Transfer and Fluid Flow, McGraw Hill, Washington, (1980).

[6] Launder, B.E., Spalding, D.B., Lectures in Mathematical Models of Turbulence. Academic Press, London, England (1972).

[7] FLUENT, Fluent 6.2 User's guide. Fluent Inc., Lebanon, NH, (2005).

[8] Sinha, S. L., Arora, R. C, and Roy, Subhransu, Numerical Simulation of Two Dimensional Room Air Flow with and Without Buoyancy, Energy And Buildings, 32(1), pp. 121–129 (2000).

[9] Farhad Memarzadeh, Andrew P. Manning, Comparison of Operating Room Ventilation Systems in the Protection of the Surgical Site.

[10] Hinds, W. C., Aerosol Technology, Properties, Behavior, and Measurement of Airborne Particles. Wiley, New York, (1982).

[11] GAMBIT 2.2 Tutorial Guide, September, (2004).